

The design of new photochromic polymers incorporating covalently or ionically linked spiropyran/polyoxometalate hybrids

Irene Bazzan,^a Patricia Bolle,^b Olivier Oms,^{*a} Hanène Salmi,^c Nadine Aubry-Barroca,^c Anne Dolbecq,^a H el ene Serier-Brault,^b R emi Dessapt,^{*b} Philippe Roger,^{*c} and Pierre Mialane^a

^aInstitut Lavoisier de Versailles, UMR 8180, Universit  Paris-Saclay, Universit  de Versailles Saint-Quentin en Yvelines, 45 Avenue des Etats-Unis, 78035 Versailles cedex (France).

^bInstitut des Mat riaux Jean Rouxel (IMN), Universit  de Nantes, CNRS, 2 rue de la Houssini re, BP 32229, 44322 Nantes cedex 3, France.

^cInstitut de Chimie Mol culaire et des Mat riaux d'Orsay (ICMMO), UMR 8182, Universit  Paris Sud, CNRS, Universit  Paris-Saclay, 91405 Orsay, France.

Supplementary Figures and Table:

Figure S1 : ¹³C NMR spectrum of (TBA)₃[**SP-POM-MA**].

Figure S2 : ¹H NMR spectrum of (TBA)₃[**SP-POM-MA**].

Figure S3 : ATR-IR spectra of (TBA)₃[**SP-POM-NH₂**] and (TBA)₃[**SP-POM-MA**].

Figure S4 : ESI/MS spectrum of (TBA)₃[**SP-POM-MA**].

Figure S5 : ¹H NMR spectrum of **poly(SP-POM-MA-co-MA)**.

Figure S6 : ATR-IR spectra of PMMA and **poly(SP-POM-MA-co-MA)**.

Figure S7 : SEC HPLC volume of elution of **poly(SP-POM-MA-co-MA)**.

Figure S8 : XPS analysis of PMMA and **poly(SP-POM-MA-co-MA)**.

Figure S9 : ATR-IR spectra of polyDMAEMA and polyDMAEMA⁺.

Figure S10 : ¹H NMR spectrum of polyDMAEMA.

Figure S11: SEC HPLC volume of elution of polyDMAEMA.

Figure S12 : ^1H NMR spectrum of polyDMAEMA⁺.

Figure S13 : ^1H NMR spectrum of **poly(SP-POM-SP-DMAEMA⁺)**.

Figure S14 : XPS analysis of polyDMAEMA⁺.

Figure S15 : ATR-IR spectra of polyDMAEMA⁺ and **poly(SP-POM-SP-DMAEMA⁺)**.

Figure S16 : Kubelka-Munk transformed reflectivity *vs* wavelength of **poly(SP-POM-MA-co-MA)** and **poly(SP-POM-SP-DMAEMA⁺)**.

Figure S17 : Photochromic effect of **poly(SP-POM-MA-co-MA)** and temporal evolution of its photogenerated absorption.

Table S1 : Photochromic kinetic parameters at room temperature of **poly(SP-POM-MA-co-MA)** and **SP-POM-NH₂-mix-PMMA**.

Experimental section

NMR spectra were recorded at 298 K on a Bruker Advance 300 spectrometer operating at 300 MHz for ^1H and 50 MHz for ^{13}C nuclei. Chemical shifts are expressed in parts per million (ppm) downfield from internal TMS. The following abbreviations are used: s, singlet; d, doublet; t, triplet; m, multiplet.

Infrared spectra (ATR) were recorded on an IRFT Nicolet 6700 apparatus. Relative intensities are given after the wavenumber as vs = very strong, s = strong, m = medium, w = weak, sh = shoulder, br = broad.

Elemental analyses were performed by the Service de Microanalyse of CNRS, 91198 Gif-sur-Yvette, France.

TGA experiments were performed with a Seiko TG/DTA 320 thermogravimetric balance (2°C/min, under N_2 atmosphere).

Electrospray ionization (ESI) mass spectra were recorded on a Xevo QToF WATERS (quadrupole-time-of-flight) instrument. The temperature of the source block was set to 120 °C, and the desolvation temperature to 200 °C. A capillary voltage of 1 kV was used in the negative scan mode, and the cone voltage was set to 10 V to control the extent of fragmentation of the identified species. Mass calibration was performed using a solution of sodium formate in water:acetonitrile (2:8) from m/z 50 to 3000. Sample solutions 50 $\mu\text{mol/L}$ in acetonitrile were injected via syringe pump directly connected to the ESI source at a flow rate of 20 $\mu\text{L/min}$.

XPS measurements were performed on a K-Alpha spectrometer from ThermoFisher, equipped with a monochromated X-ray Source (Al K alpha, 1486.6 eV). For all measurements a spot size of 400 μm was employed. The hemispherical analyzer was operated in CAE (Constant Analyzer Energy) mode, with a pass energy of 200 eV and a step of 1 eV for the acquisition of surveys spectra, and a pass energy of 50 eV and a step of 0.1 eV for the acquisition of high resolution spectra. A “dual beam” flood gun was used to neutralize the charge build-up. The spectra obtained were treated by means of the “Avantage” software provided by ThermoFisher. A Shirley type background subtraction was used and the peak areas were normalized using the Scofield sensitivity factors in the calculation of elemental compositions. The binding energies were calibrated against the C1s binding energy set at

284.8 eV. The peaks were analyzed using mixed Gaussian-Lorentzian curves (70% of Gaussian character).

Diffuse reflectance spectra were collected at room temperature on a finely ground sample with a Cary 5G spectrometer (Varian) equipped with a 60 mm diameter integrating sphere and computer control using the “Scan” software. Diffuse reflectance was measured from 250 to 1550 nm with a 2 nm step using Halon powder (from Varian) as reference (100% reflectance). The reflectance data were treated by a Kubelka-Munk transformation¹ to obtain the corresponding absorption data. The photocoloration and fading kinetics were quantified by monitoring the temporal evolution of the photogenerated absorption $Abs^{580}(t)$ defined as $Abs^{580}(t) = -\log(R^{580}(t)/R^{580}(0))$, where $R^{580}(t)$ and $R^{580}(0)$ are the reflectivities at the time t and at $t = 0$, respectively. For the coloration kinetics, the samples were irradiated with a Fisher Bioblock labosi UV lamp ($\lambda_{ex} = 365$ nm, $P = 6W$) at a distance of 50 mm. $Abs^{580}(t)$ vs. t plots have been fitted according to a biexponential rate law $Abs^{580}(t) = (A_1 + A_2) - A_1 \exp(-k^c_1 t) - A_2 \exp(-k^c_2 t)$, with k^c_1 and k^c_2 the extracted coloration rate constants. For the bleaching processes, the samples were first irradiated under 365 nm-UV excitation until the photoinduced absorptions reach saturation. Then, the compounds were put under Thorlabs LED Array light sources (590 nm - 1.4 W/cm²) at a distance of 100 mm. The bleaching kinetics were determined at room temperature by monitoring the temporal decays of $Abs^{580}(t)$ of samples once irradiated. $Abs^{580}(t)$ vs. t plots have been fitted according to a biexponential rate law $Abs^{580}(t) = (A_0 - A_1 - A_2) + A_1 \exp(-k^f_1 t) + A_2 \exp(-k^f_2 t)$, with k^f_1 and k^f_2 the extracted fading rate constants.

¹ Kubelka, P.; Munk, F. *Z. Techn. Physik*, 1931, **12**, 593.

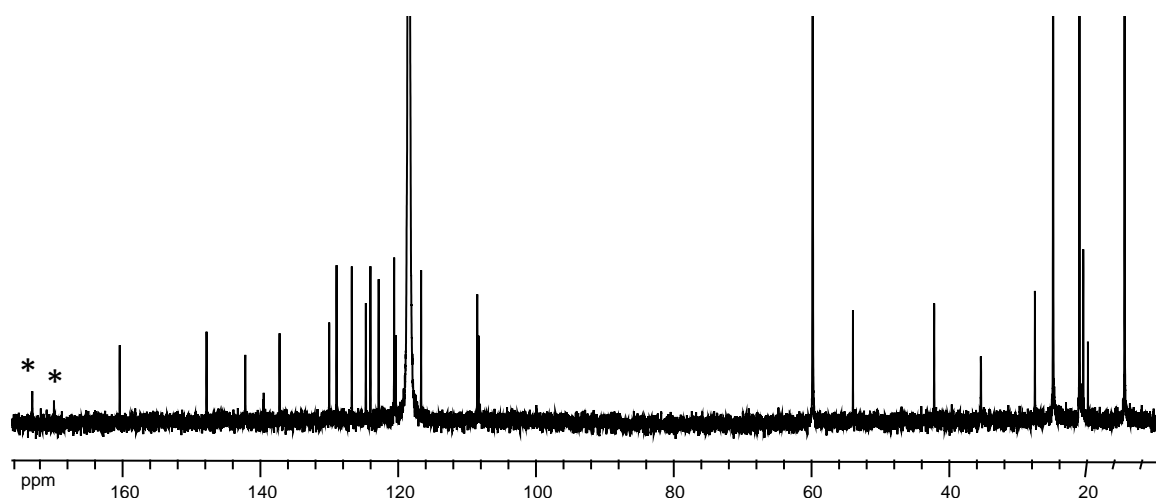


Figure S1: ^{13}C NMR spectrum in CD_3CN of $(\text{TBA})_3[\text{SP-POM-MA}]$. (*refer to the signals of two different amide functions present in the unsymmetrical hybrid POM).

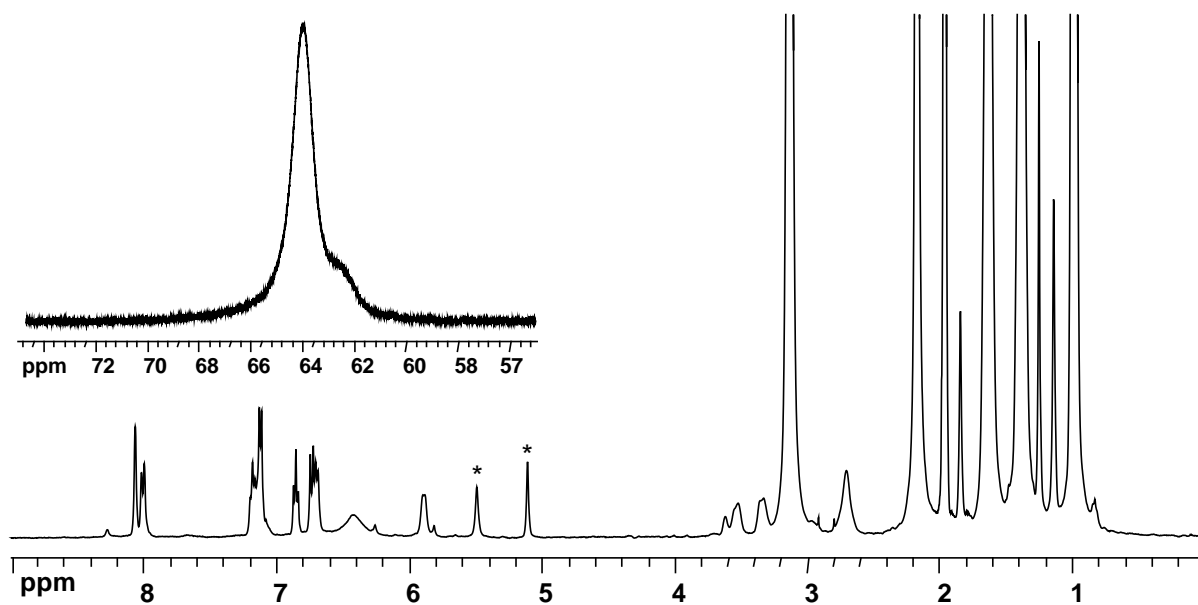


Figure S2: ^1H NMR spectrum in CD_3CN of $(\text{TBA})_3[\text{SP-POM-MA}]$ (*refer to the signals of the vinylic protons of the MA group).

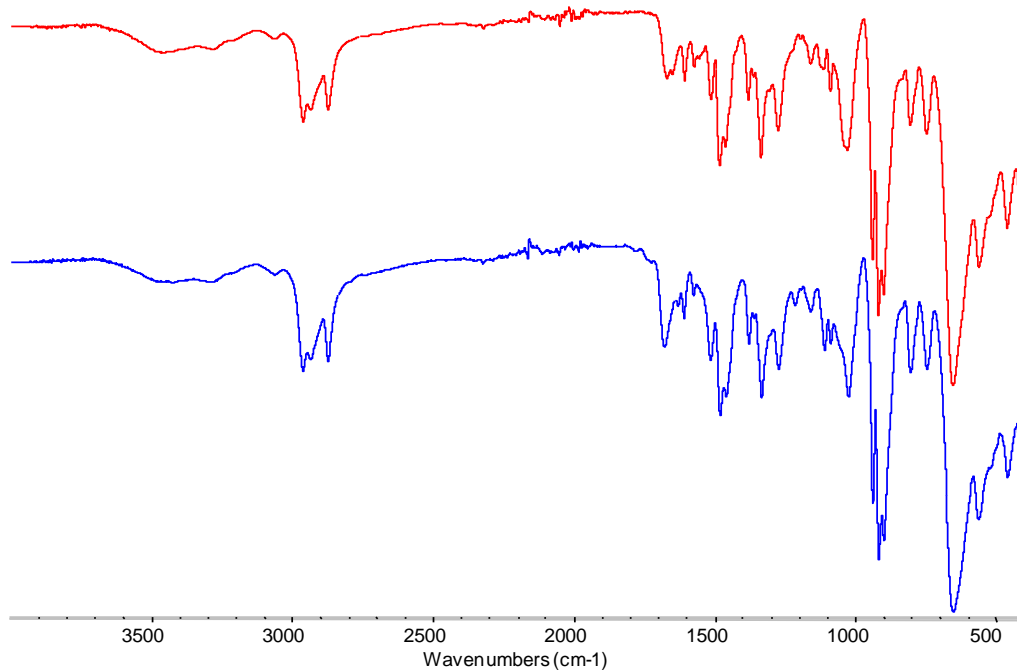
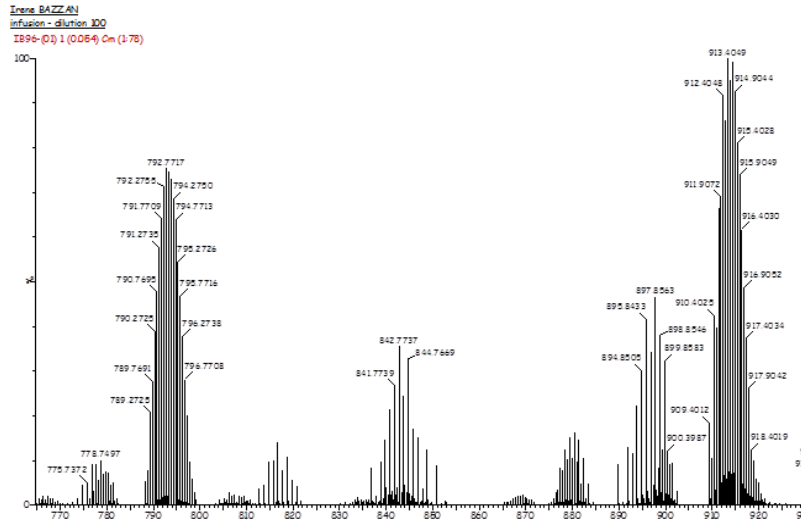
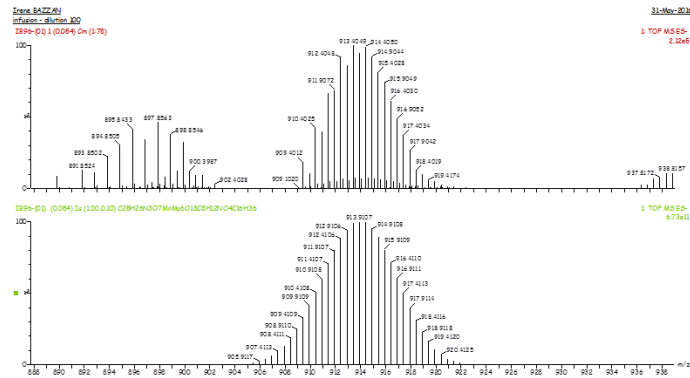


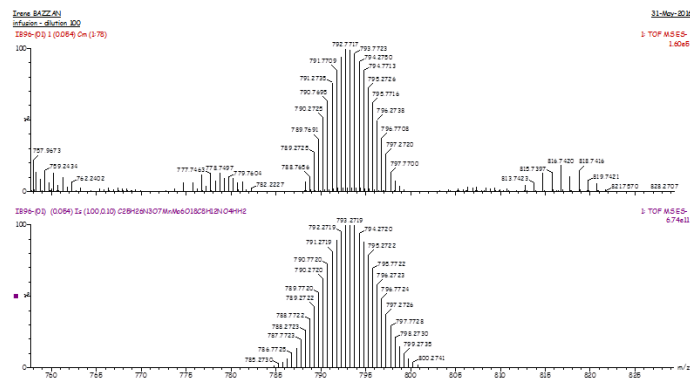
Figure S3 : ATR-IR spectra of (TBA)₃[SP-POM-NH₂] (red line) and (TBA)₃[SP-POM-MA] (blue line).



ES/MS spectrum of $(TBA)_3[SP-POM-MA]$



Top: Experimental spectrum, bottom: simulated spectrum (related to $[M+TBA]^{2-}$ signal)



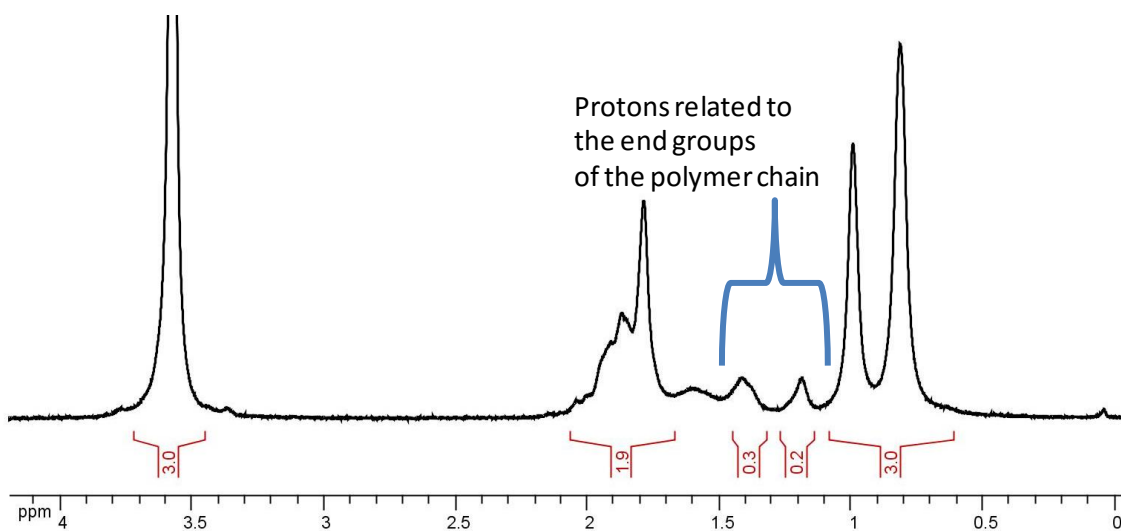


Figure S5 : ^1H NMR spectrum in CDCl_3 of **poly(SP-POM-MA-co-MA)**.

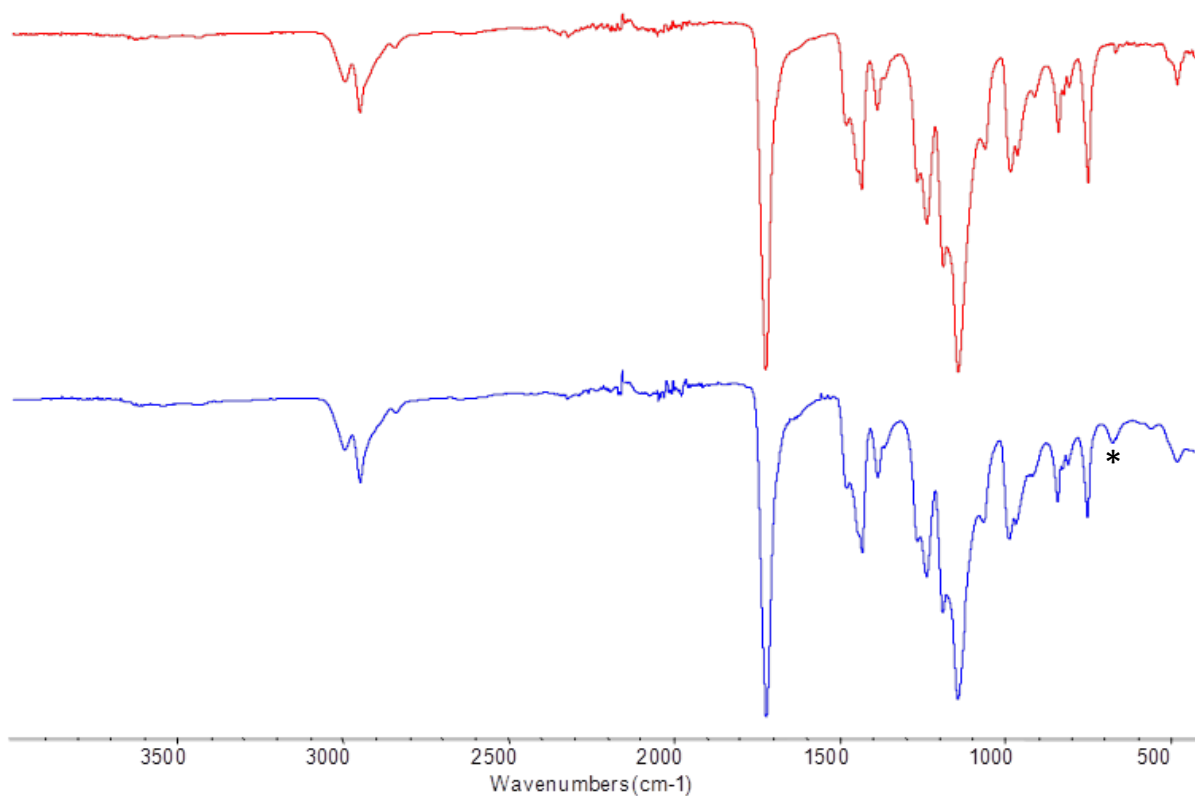


Figure S6 : ATR-IR spectra of PMMA (**red line**) and **poly(SP-POM-MA-co-MA)** (**blue line**) copolymer. (*refers to Mo-O-Mo vibration band)

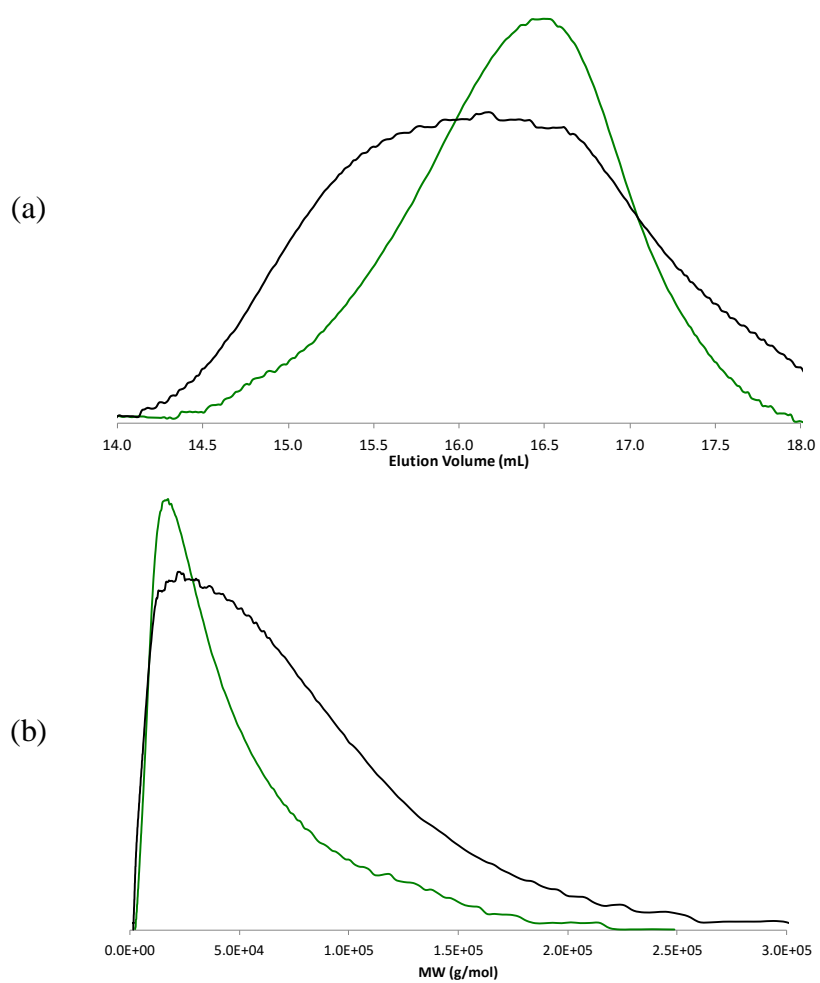


Figure S7: SEC HPLC (a) volume of elution and (b) molar weight distribution in THF eluent of PMMA (black line) and poly(SP-POM-MA-co-MA) (green line).

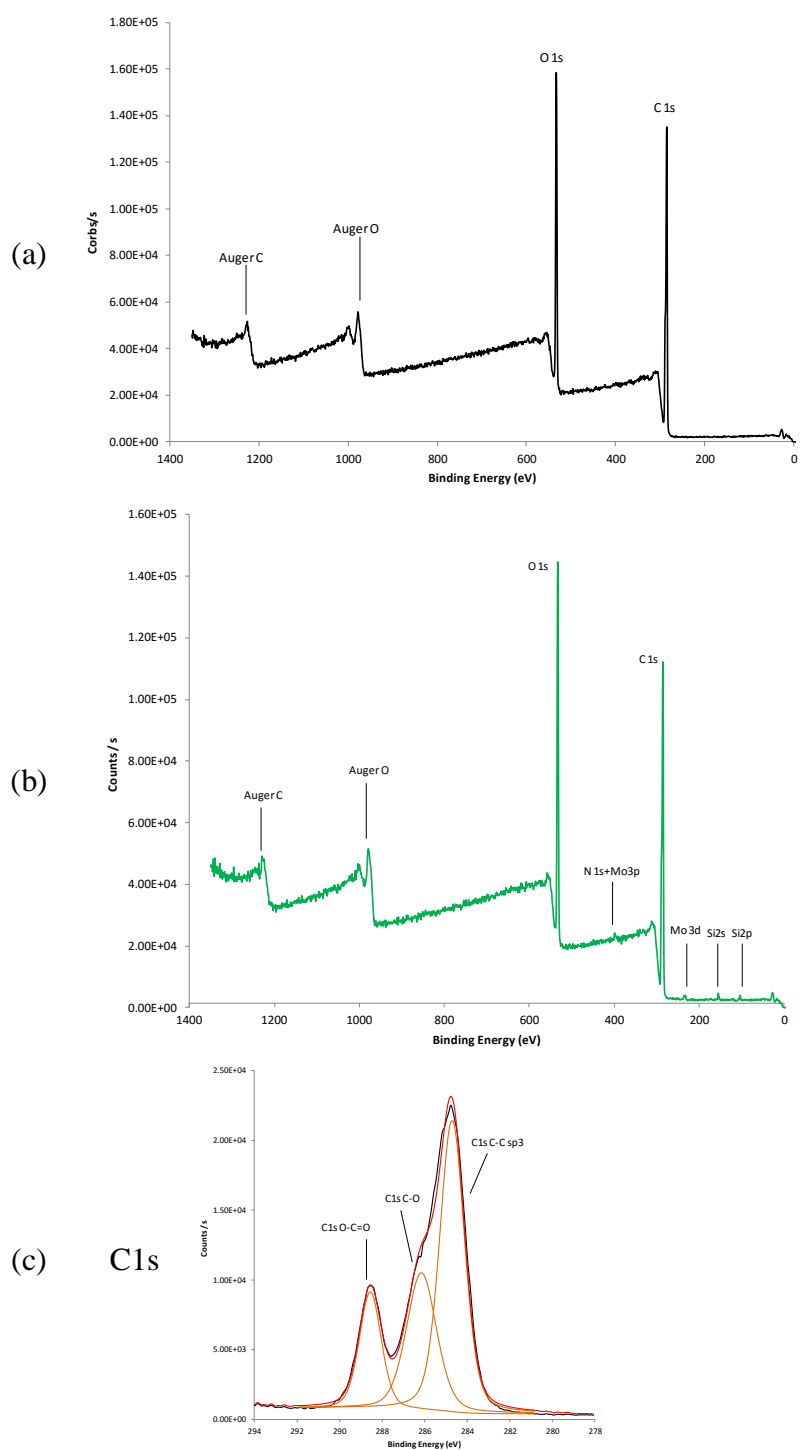


Figure S8 : Survey spectra of XPS analysis for: (a) PMMA and (b) **poly(SP-POM-MA-co-MA)**; (c) zoom for C1s energies pattern of **poly(SP-POM-MA-co-MA)**: recovered spectrum (black line) and enveloped spectrum (red line).

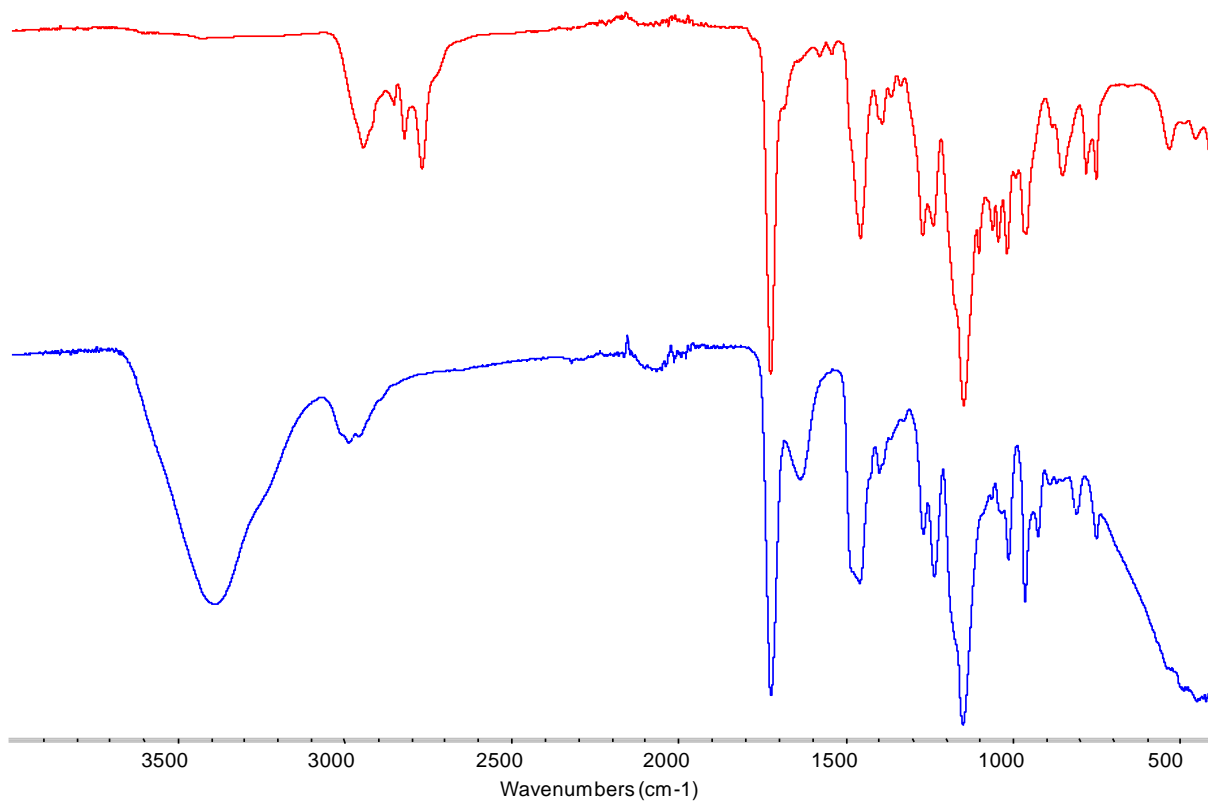


Figure S9 : ATR-IR spectra of polyDMAEMA (red line) and polyDMAEMA⁺ (blue line).

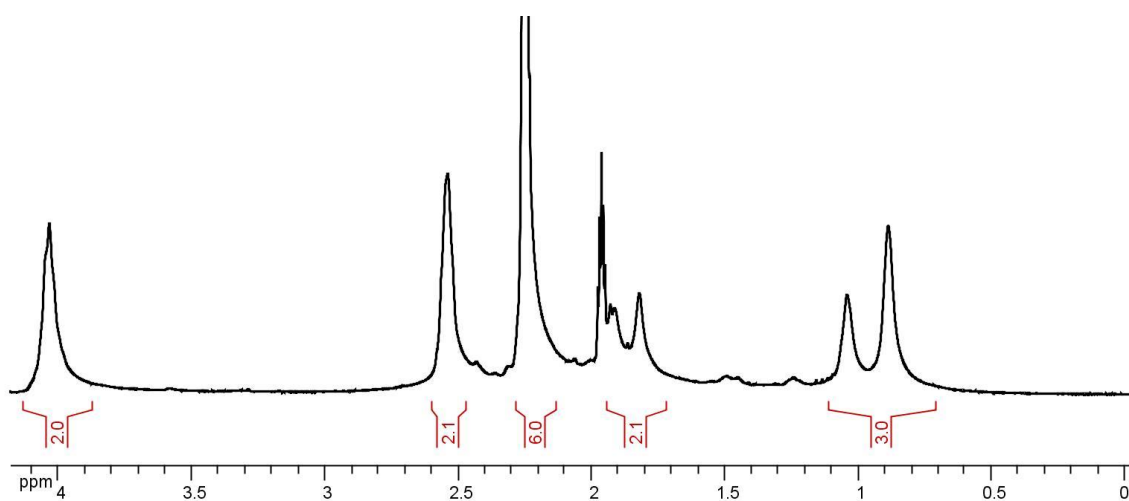


Figure S10 : ¹H NMR spectrum in CD₃CN of polyDMAEMA.

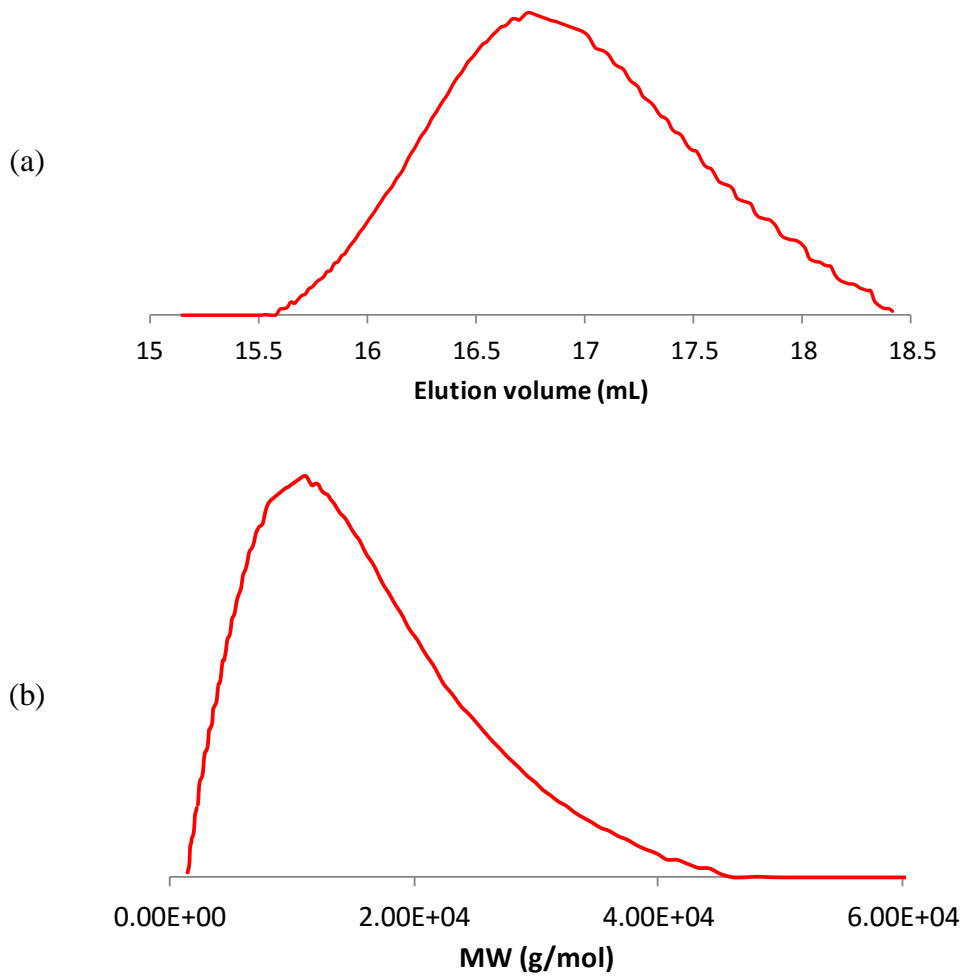


Figure S11 : SEC HPLC (a) volume of elution and (b) molar weight distribution in THF eluent of polyDMAEMA.

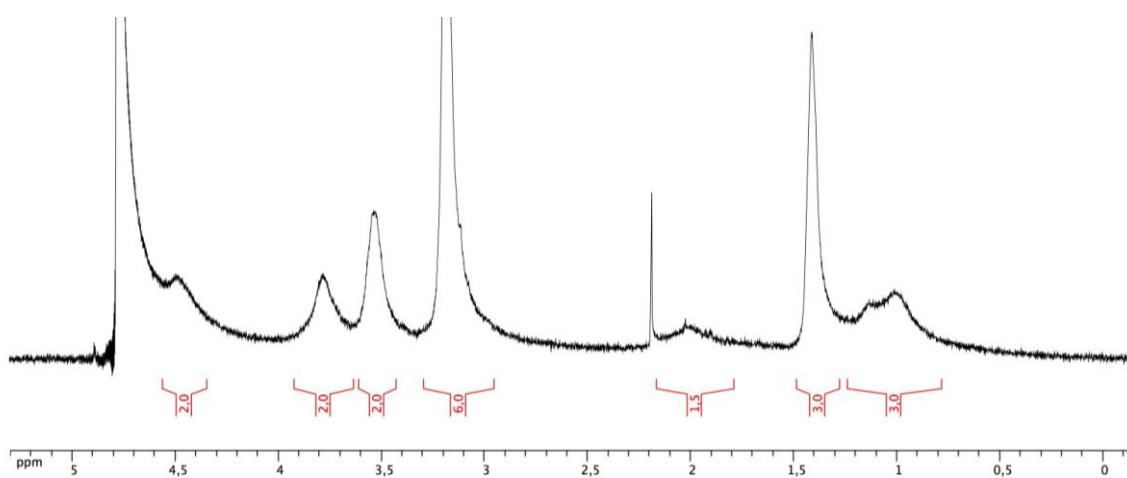


Figure S12 : ¹H NMR spectrum in D₂O of polyDMAEMA⁺.

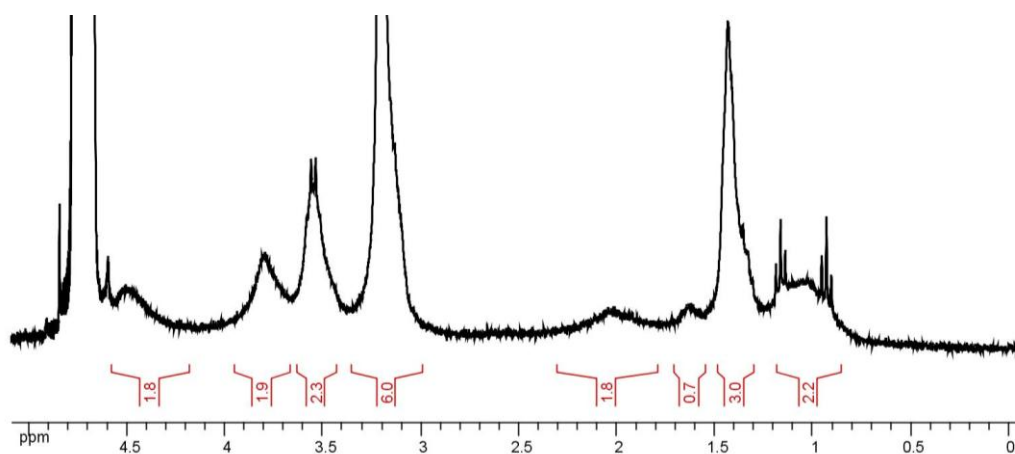


Figure S13 : ^1H NMR spectrum in D_2O of poly(SP-POM-SP-DMAEMA $^+$).

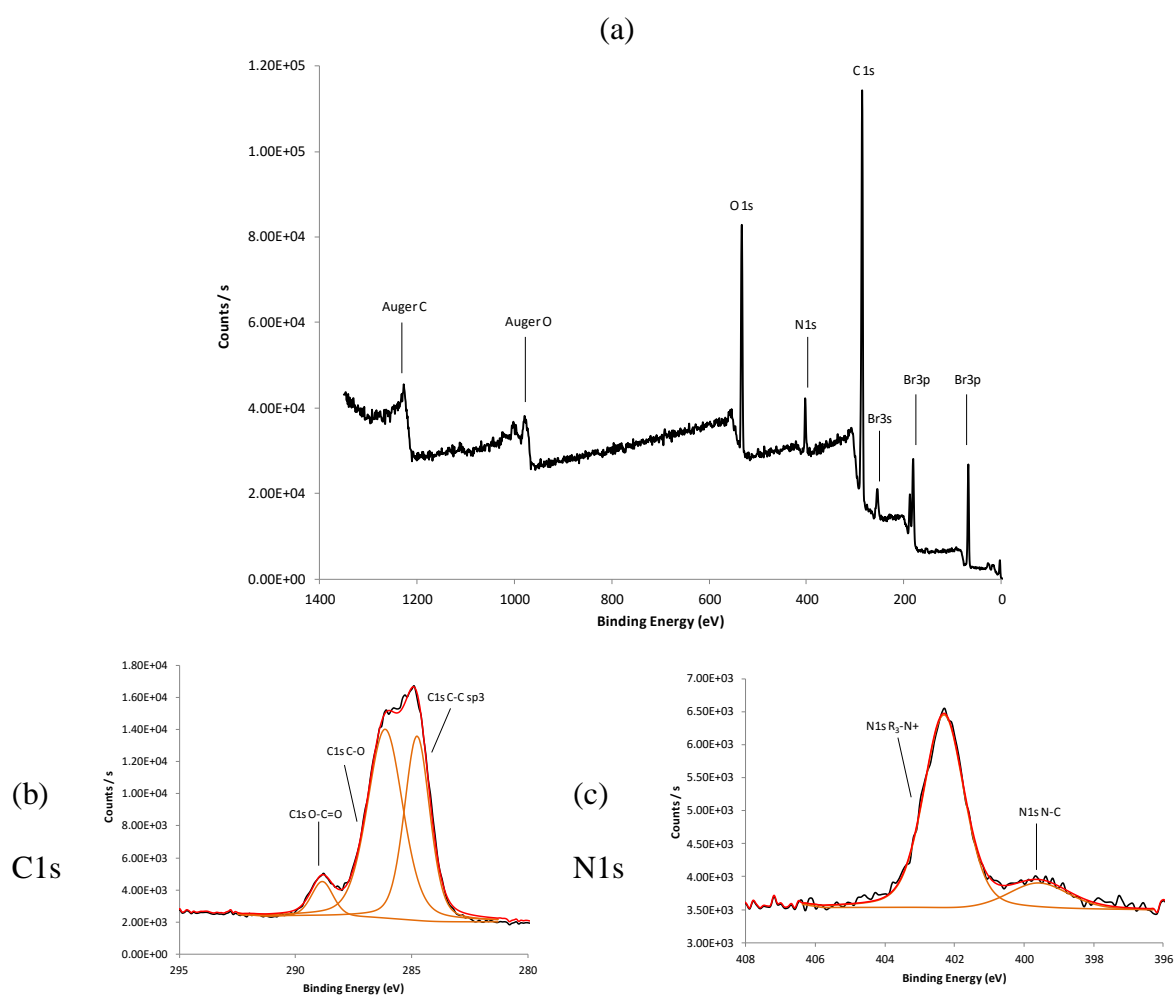


Figure S14: (a) Survey spectrum of XPS analysis for polyDMAEMA $^+$; zoom for (b) C1s and (c) N1s energies pattern (in black recovered spectrum, in red enveloped spectrum).

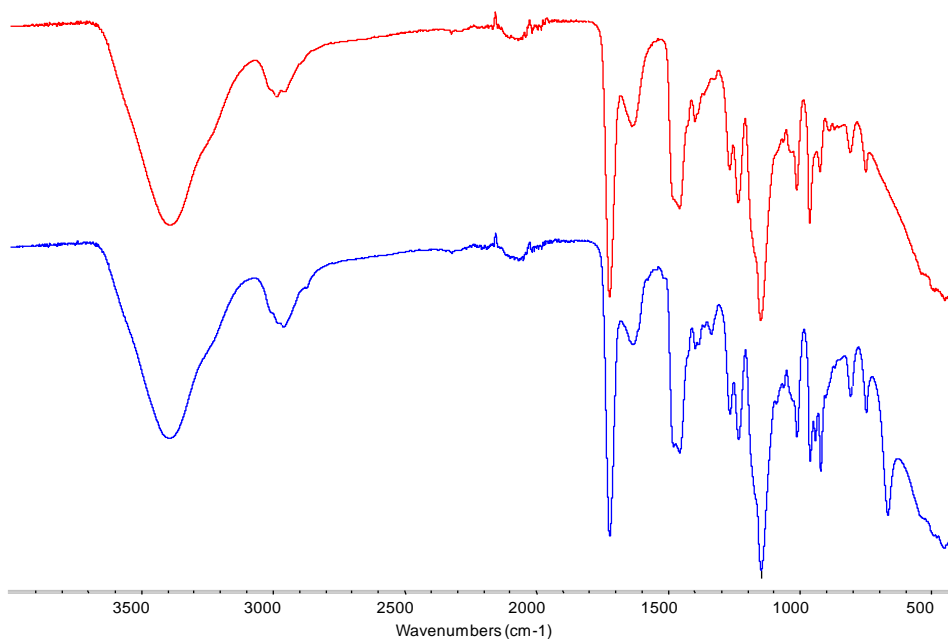


Figure S15: ATR-IR spectra of polyDMAEMA⁺ (red line) and poly(SP-POM-SP-DMAEMA⁺) (blue line).

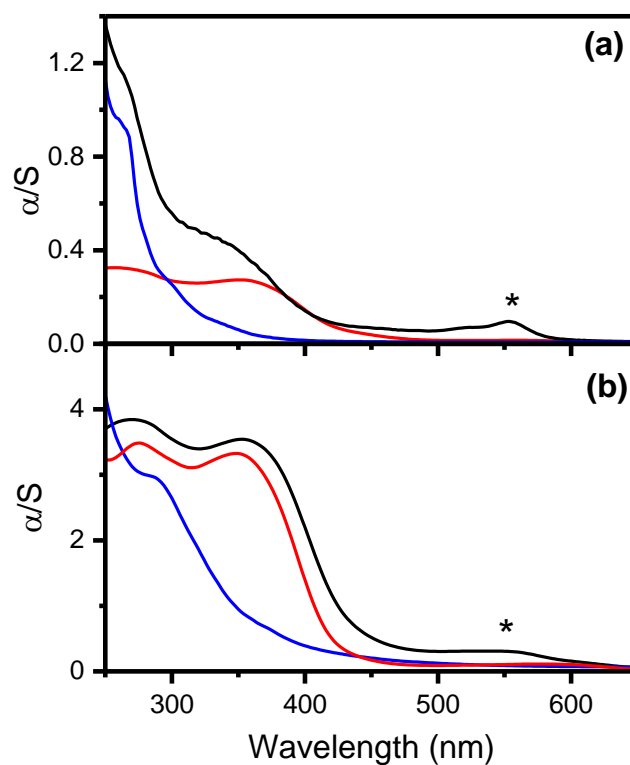


Figure S16: Kubelka-Munk transformed reflectivity vs wavelength of (a) (TBA)₃[SP-POM-NH₂] (red line), PMMA (blue line), and poly(SP-POM-MA-co-MA) (black line), (b) (TBA)₃[SP-POM-SP] (red line), polyDMAEMA⁺ (blue line) and poly(SP-POM-SP-DMAEMA⁺) (black line). The absorption band of the merocyanine coloured form is noted by an asterisk.

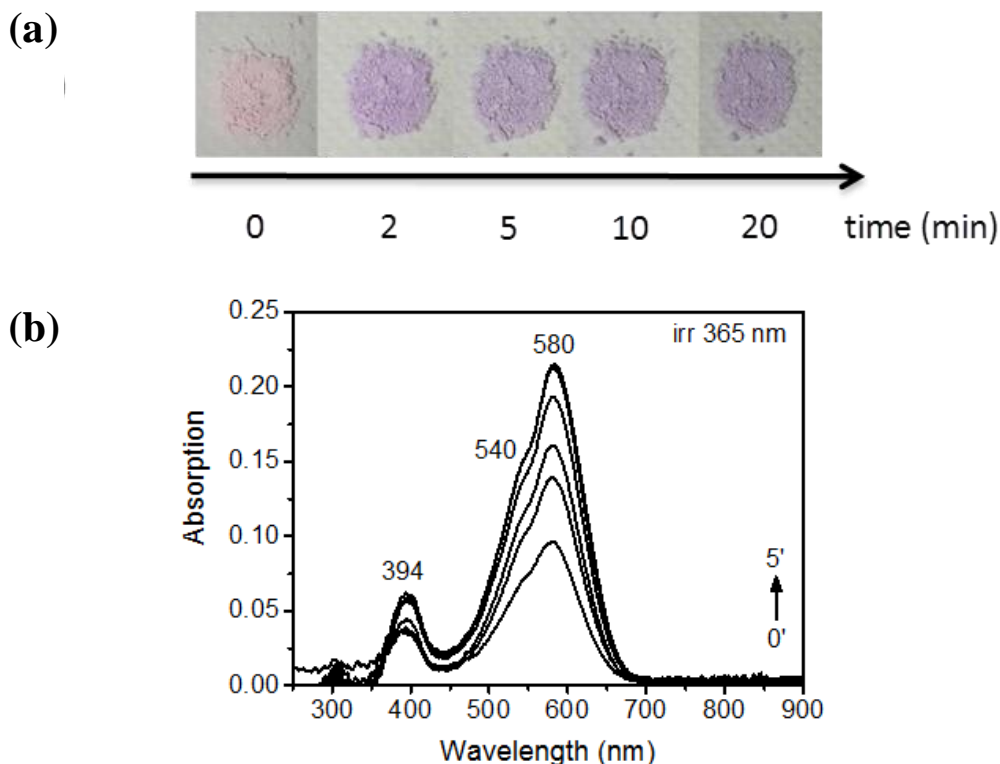


Figure S17. (a) Photographs of the powder of **poly(SP-POM-MA-co-MA)** at different time during the coloration process under 365-nm UV irradiation at room temperature. (b) Temporal evolution of the photogenerated absorption of **poly(SP-POM-MA-co-MA)** after 0, 0.166, 0.333, 0.5, 1, 2, 3, 4, and 5 min of 365 nm-UV irradiation.

Table S1. Photochromic kinetic parameters at room temperature of **poly(SP-POM-MA-co-MA)**, and **SP-POM-NH₂-mix-PMMA**.

| <i>Photocoloration process</i> | | | | | | |
|---------------------------------------|---------|---------|---|---|---------------------------|---------|
| Compound | A_1^a | A_2^a | $k^c \times 10^3 \text{ (s}^{-1}\text{)}^b$ | $k_2^c \times 10^3 \text{ (s}^{-1}\text{)}^b$ | $t_{1/2} \text{ (min)}^c$ | R^2^d |
| poly(SP-POM-MA-co-MA) | 0.091 | 0.123 | 126.4 ± 11.7 | 29.5 ± 1.7 | 0.2 | 0.9998 |
| SP-POM-NH₂-mix-PMMA | 1.215 | 0.317 | 10.5 ± 1.6 | 112.5 ± 8.6 | 0.73 | 0.9905 |

| <i>Thermal fading process in the dark</i> | | | | | | | |
|---|---------|---------|---------|---|---|---------------------------|---------|
| Compound | A_0^a | A_1^a | A_2^a | $k_1^f \times 10^3 \text{ (s}^{-1}\text{)}^b$ | $k_2^f \times 10^3 \text{ (s}^{-1}\text{)}^b$ | $t_{1/2} \text{ (min)}^c$ | R^2^d |
| poly(SP-POM-MA-co-MA) | 0.214 | 0.062 | 0.041 | 0.5 ± 0.1 | 8.4 ± 1.3 | 7.1 | 0.9975 |
| SP-POM-NH₂-mix-PMMA | 1.552 | 0.047 | 0.008 | 0.08 ± 0.01 | 2.3 ± 0.6 | 108.3 | 0.9976 |

| <i>Fading process under visible-light irradiation ($\lambda_{ex} = 590 \text{ nm}$)</i> | | | | | | | |
|--|---------|---------|---------|---|---|---------------------------|---------|
| Compound | A_0^a | A_1^a | A_2^a | $k_1^f \times 10^3 \text{ (s}^{-1}\text{)}^b$ | $k_2^f \times 10^3 \text{ (s}^{-1}\text{)}^b$ | $t_{1/2} \text{ (min)}^c$ | R^2^d |
| poly(SP-POM-MA-co-MA) | 0.214 | 0.105 | 0.074 | 68.7 ± 8.5 | 2.5 ± 0.4 | 0.4 | 0.9925 |
| SP-POM-NH₂-mix-PMMA | 1.541 | 1.373 | 0.035 | 0.2 ± 0.0 | 84.5 ± 129.4 | 62.5 | 0.9974 |

^aThe $\text{Abs}^{580}(t)$ vs t plots were fitted as $\text{Abs}^{580}(t) = (A_1 + A_2) - A_1 \exp(-k^c t) - A_2 \exp(-k_2^c t)$ for the coloration process and as $\text{Abs}^{580}(t) = (A_0 - A_1 - A_2) + A_1 \exp(-k_1^f t) + A_2 \exp(-k_2^f t)$ for the fading ones. ^bColoration (k^c) and fading (k^f) rate constants. ^cFor the coloration process, the half-life time $t_{1/2}$ is defined as the UV irradiation time required for $\text{Abs}^{580}(t)$ to reach half of its maximum value. For the fading ones, $t_{1/2}$ is defined as the irradiation time required for $\text{Abs}^{580}(t)$ to reach the $A_0 - (A_1 + A_2)/2$ value. ^dRegression coefficient for the $\text{Abs}^{580}(t)$ vs t plots.